Roaming Dynamics in Acetone Dissociation†

Vasiliy Goncharov, Nuradhika Herath, and Arthur G. Suits*

Department of Chemistry, Wayne State University, Detroit, Michigan 48202

Received: March 24, 2008; Revised Manuscript Received: May 9, 2008

DC slice imaging has been employed to study the photodissociation dynamics of acetone at 230 nm, with detection of the CO photoproduct via the $B\ (v' = 0)\ ^1\Sigma^+ \leftarrow X\ (v'' = 0)\ ^1\Sigma^+$ transition. A bimodal translational energy distribution observed in the CO fragments points to two distinct dissociation pathways in the 230 nm photolysis of acetone. One pathway results in substantial translational energy release ($E_{ave} \approx 0.3$ eV) along with rather high rotational excitation (up to $J'' = 50$) of CO, and is attributed to the thoroughly investigated stepwise mechanism of bond cleavage in acetone. The other dissociation pathway leads to rotationally cold CO ($J'' = 0-20$) with very little energy partitioned into translation ($E_{ave} \approx 0.04$ eV) and in this way it is dynamically similar to the recently reported roaming mechanism found in formaldehyde and acetaldehyde dissociation. We ascribe the second dissociation pathway to an analogous roaming dissociation mechanism taking place on the ground electronic state following internal conversion. For acetone, this would imply highly vibrationally excited ethane as a coproduct of rotationally cold CO, with the ethane formed above the threshold for secondary decomposition. We estimate that about 15% of the total CO fragments are produced through the roaming pathway. Rotational populations were obtained using a new Doppler-free method that simply relies on externally masking the phosphor screen under velocity map conditions in such a way that only the products with no velocity component along the laser propagation direction are detected.

I. Introduction

The "roaming mechanism" has recently emerged as a new pathway in unimolecular decomposition.[1–9] This phenomenon, initially reported and characterized in detail in studies of formaldehyde photodissociation, involves near-dissociation of a molecule to radical products, followed by intramolecular abstraction to give, instead, highly vibrationally excited closed-shell products. It is significant in that it represents an extreme example of a nonminimum energy path (MEP) reaction,[10–13] one that bypasses the nominal transition state geometry for the reaction and challenges the normal Transition State Theory description of the reaction. Recent experimental and theoretical studies have now confirmed a similar process in acetaldehyde photodissociation,[7–9,14] and in that case it is a methyl radical that is the "roaming" species. These roaming reactions may be written

$$H_2CO \rightarrow (H + HCO) \rightarrow H_2^{\ddagger} + CO \qquad (1)$$

$$CH_3CHO \rightarrow (CH_3 + HCO) \rightarrow CH_4^{\ddagger} + CO \qquad (2)$$

In this paper, we present evidence for an analogous roaming contribution in the ultraviolet photodissociation of acetone through the S_1 electronic state, implying highly vibrationally excited ethane as a coproduct:

$$CH_3COCH_3 \rightarrow (CH_3 + CH_3CO) \rightarrow C_2H_6^{\ddagger} + CO \qquad (3)$$

The fate of this hot ethane product will be considered further below.

The photochemistry of acetone is among the most thoroughly studied of any polyatomic molecule, with hundreds of studies ranging from classical flash photolysis and nanosecond laser studies[15–21] to a dizzying array of recent femtosecond studies[16,22–31] as well as extensive theoretical work.[28,32–34] It is perhaps surprising that a unified picture of its dissociation dynamics has not yet emerged. This is likely a testament to the complexity of the problem and the changing dynamics with excitation energy as key surface crossings are accessed. Nevertheless, some conclusions are widely accepted, and the schematic energy diagram in Figure 1 is useful as we review them. Excitation in the first absorption band is from a nonbonding oxygen atom orbital to a π^* orbital leading to the S_1 surface which has a pyramidal central carbon. At the long wavelength end of the absorption, dissociation occurs via C−C bond fission following intersystem crossing (ISC) to the triplet surface (T_1), as long as the energy exceeds that of the triplet barrier, 4.05 eV (305.8 nm). At higher excitation energies, e.g., 248 nm, the triplet dissociation (the "T_1" pathway) can leave enough excitation in the remaining acetyl radical for it to undergo secondary decomposition. The acetyl radical itself has an exit barrier of ∼0.4 eV,[35] so that the translational energy distribution for the CO product of this secondary decomposition peaks away from zero.[20] However, some recent isotopic labeling experiments have complicated this picture somewhat.[36] Mercury lamp photolysis of mixtures of acetone and perdeuteroacetone in a cell at energies below the triplet barrier were found to give rise to a significant fraction (∼25%) of ethane molecules via an *intramolecular* pathway. The implications of this will be considered further below.

The dissociation dynamics following excitation to S_2 in the intense second absorption band around 193 nm (an n−3s Rydberg excitation) have also received a great deal of attention,[17–20,25,29] and much of the discussion is relevant here as well. Pilling and co-workers studied the reaction via end-product analysis and time-resolved absorption in a cell at 300 and 600 K.[19] They observed ethane and CO as dominant products, but based on radical scavenging experiments con-

† Part of the "Stephen R. Leone Festschrift".

* To whom correspondence should be addressed. E-mail: asuits@chem.wayne.edu.

10.1021/jp802534r CCC: $40.75
Published on Web 06/28/2008

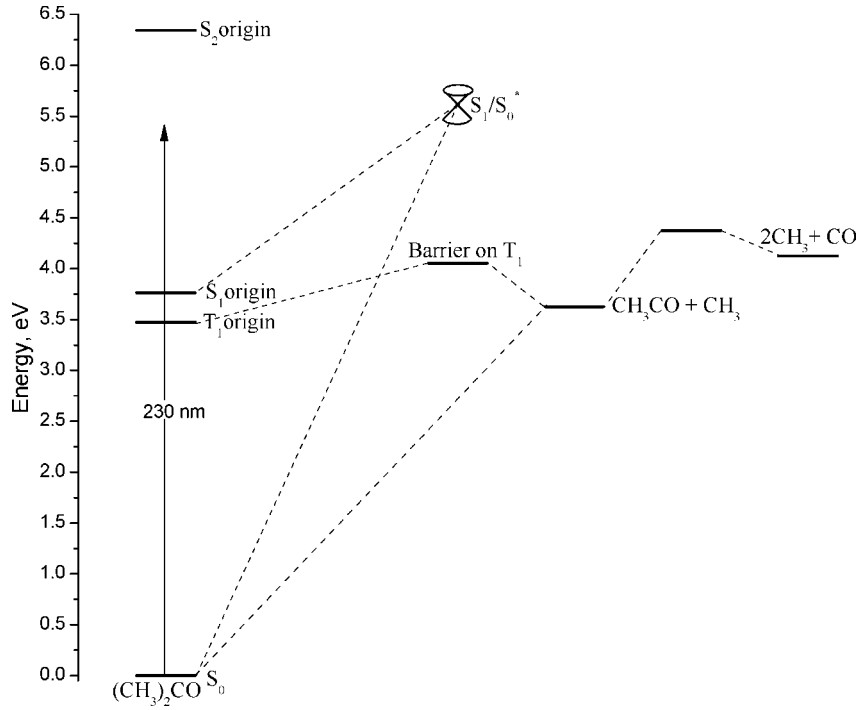

Figure 1. Energy diagram for photodissociation of acetone at 230 nm.

cluded that reaction to produce CO and two methyl radicals accounted for 95% of the overall photolysis, with H and CH_4 elimination accounting about equally for the remaining 5%. North et al.,[20] using photofragment translational spectroscopy, saw a single CH_3 time-of-flight peak but were able to fit it by assuming two components, one of which was little changed from their result for the 248 nm case. They concluded that the S_2 dissociation also proceeded mainly by internal conversion to S_1, with the S_1 dynamics following the same decomposition path, via the triplet, as at 248 nm. At 193 nm, however, essentially all of the acetyl undergoes secondary decomposition. Zewail and co-workers[29,37] have argued instead that in this energy region, direct decomposition on S_1 may occur via a transition state that correlates to a linear acetyl radical in the *A* state (essentially one component of a Renner-Teller pair that is anyway degenerate at the linear geometry). This is the "S_1 mechanism", since championed by Cheng et al.[29–31] We should note that the acetyl radical is then believed to relax immediately to the ground state, so that the subsequent secondary decomposition would be essentially the same as that on the T_1 pathway.

One feature of this discussion that has not received much attention is the S_1/S_0 crossing, shown in Figure 1 and identified in calculations from Liu et al.[32] and from Zewail and co-workers.[28] This conical intersection (CI) is very near, both in energy and in geometry, to the S_1 TS. We should thus have in mind that events that undergo dissociation via the S_1 pathway are likely accompanied by others that lead to the ground-state via internal conversion (IC) at this CI. Dissociation on the ground-state can then occur without a barrier to give CH_3 + acetyl. The absence of a barrier is key for the roaming intepretation below. In short, the S_1 and S_0 surfaces are mixed at these geometries. Key points in sorting through all these issues are the locations of the CIs and crossings among the relevant surfaces, summarized here: The T_1 barrier is 4.05 eV, the S_1/S_0 CI is 5.6 eV and the S_1 barrier is 5.8 eV. Zewail and co-workers have also explored direct decomposition on the S_2 surface,[34] but the barrier is ~7.1 eV, so that pathway is not relevant for dissociation at 193 nm or below.

In this study we present DC slice imaging[38] of state-selected CO molecules following dissociation of acetone around 230nm. The imaging results are combined with Doppler-free resonant multiphoton ionization (REMPI) spectra of the CO product obtained using a new masked velocity mapping approach, to reveal a surprising aspect of acetone photodissociation dynamics in the high-energy range of the S_1 absorption.

II. Experimental Section

A supersonic beam, 5% of acetone seeded in Ar, produced by a General valve with the backing pressure of 2 atm and pulse duration ~200 μs, was introduced into a differentially pumped velocity map imaging apparatus, which has been described elsewhere.[38] The background pressures in a source and detector chambers with the beam on were $\sim 2 \times 10^{-6}$ and $\sim 2 \times 10^{-7}$ torr, respectively. The valve and inlet tubing were kept at 55 °C to minimize acetone condensation on the walls and cluster formation in the molecular beam. In order to accomplish a laser line width limited resolution and avoid scanning through broad Doppler profiles of the ground-state CO rotational lines, a two-color reduced-Doppler (TCRD) approach was utilized, as previously described.[39] For this purpose, two identical and independently tunable UV laser beams were generated by sum-frequency mixing of the third harmonic of seeded Nd:YAG lasers (Spectra Physics, model: Quanta-Ray PRO 250) and a fundamental output of dye lasers (Sirah Laser- and Plasmatechnik GmbH, model: PrecisionScan) pumped by the second harmonic of the same Nd:YAG laser. The UV laser beams were temporally overlapped and sent into the detector chamber in opposite directions. The experiment was designed in such a way that a photon from either laser could cause photolysis of acetone, but only a pair of photons, one from each laser, led to resonant ionization of CO products.[39,40] For this, the wavelength of one laser was fixed near the resonance and the wavelength of the other was set so that the combined energy of two photons was fixed on a resonance of the Q-branch of the (2 + 1) REMPI $B\ (v' = 0)\ ^1\Sigma^+ \leftarrow X\ (v'' = 0)\ ^1\Sigma^+$ transition. We found that the

laser fluence of ~2 mJ/mm^2 was sufficient to photodissociate acetone and resonantly ionize CO. The resulting ions were accelerated toward a 120 mm microchannel plate detector coupled to a phosphor screen, monitored both with a CCD camera and a photomultiplier tube. The DC slice imaging approach was employed along with our IMACQ Megapixel imaging software, as previously reported,[38,41] for image acquisition and analysis. REMPI spectra were recorded by collecting the signal from the photomultiplier tube while stepping the laser wavelength across the $B \leftarrow X$ transition of CO and measuring the wavelength of the dye laser at each step with a digital wavelength meter (WaveMaster, Coherent, ± 0.1 cm^{-1} accuracy, ± 0.02 cm^{-1} resolution). During all experiments, extra care was taken to sample only the very early part of the molecular beam expansion where no clusters are expected. One of the products of the photolysis of acetone clusters is an acetone ion with nonzero translational energy. Those ions were detected at the tail of the supersonic beam expansion only when the acetone to Ar ratio was increased to ~1:1. Under the conditions of the experiment, CO^+ was the only ion poduced to any significant extent, and there was no CO^+ signal when the laser was tuned away from the resonance.

III. Results

The images and translational energy distributions of the ground-state CO in various degrees of rotational excitation ($J'' = 4, 8, 14, 30$) produced from the photolysis of acetone at 230 nm are given in Figure 2. As can be qualitatively inferred from the images, the available energy is partitioned into CO fragments in two distinct ways. A rather broad translational energy distribution is seen in a wide range of CO product rotational levels and appears to be more prominent with larger J''. In addition, some images for the first few rotational levels of CO also show a very sharp peak at low translational energy release. However, as J'' increases the broad distribution rapidly becomes dominant. The same bimodal distribution can be observed and characterized on a quantitative basis from the corresponding translational energy distributions (see Figure 2). We should note that, in contrast to the customary manner of presenting the total translational energy release, here we show the translational energy for the detected CO fragment only, as the CO may arise from a mixture of two-body and three-body dissociation events. The average translational energies $\langle E_T \rangle$ obtained from the $P(E_T)$ distributions for various rotational levels of CO are given in Table 1. In order to estimate the branching of the two different energy partitioning modes, $P(E_T)$ curves were fitted to the general expression of the following form[42]

$$P(E_T)_{\mathbf{bimodal}} = P(E_T)_{\mathbf{sharp}} + P(E_T)_{\mathbf{broad}} = A \cdot (E_T)^i \cdot (1 - E_T)^j + B \cdot (E_T)^m \cdot (1 - E_T)^n \quad \text{(I)}$$

where the power coefficient n was kept fixed for all rotational levels as the tail of the $P(E_T)_{\text{bimodal}}$ has no contribution from $P(E_T)_{\text{sharp}}$. These expressions provide a simple way of decomposing the energy distributions, but we do not mean to draw any direct mechanistic inferences from this fitting or the value of these coefficients. Even though other coefficients (i, j, and m) were varied, the resulting parameters turned out to be almost the same for different J'' as well. Only the weighting parameters (A and B) changed significantly, which is not surprising as the translational energy distributions in this case (e.g., coming off the acetyl barrier) will not be expected to change dramatically with J''. The resulting curves are given in Figure 2. The individual fitted distributions are shown in red, whereas the total distribution is given in blue. As can be seen, the simulated curves are well fitted to the experimental data points. The branching for different rotational levels is summarized in the Table 1. The overall branching for the ground-state CO ($v'' = 0$) can be obtained if the relative rotational populations are known, which in turn can be estimated from the rotational line intensities. For this purpose TCRD REMPI spectra of the Q-branch B←X transition were initially recorded. Surprisingly, the spectra exhibited a very well pronounced sinusoidal ionization probability superimposed on the line intensity profile that precluded further rotational state distribution analysis. More details on this effect will follow.[43] In the meantime, we developed a new, Doppler-free method, which, unlike TCRD[39] or conventional Doppler-free methods, requires only one laser beam and does

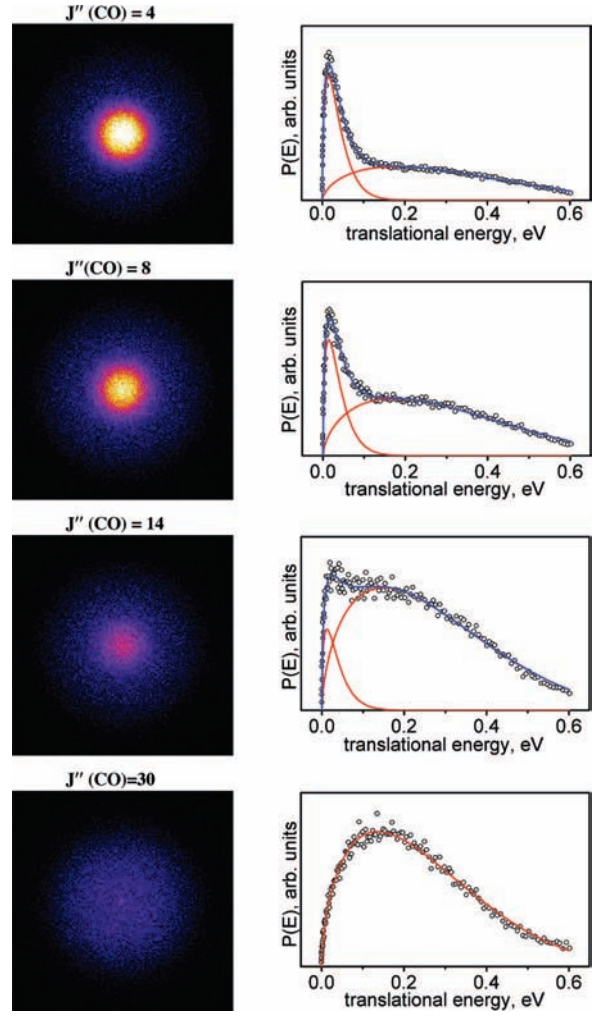

Figure 2. DC sliced images and translational energy release of the CO photofragments from the 230 nm photolysis of acetone.

TABLE 1: Characteristics of Bimodal Distribution in CO Photofragments

J''	$\langle E_T \rangle$, total eV	$\langle E_T \rangle$, broad, eV	$\langle E_T \rangle$, sharp, eV	branching to sharp, %	relative rotational population
4	0.23	0.310(6)	0.038(3)	30	0.031
6	0.24	0.310(6)	0.038(3)	26	0.042
8	0.26	0.310(6)	0.038(3)	19	0.038
10	0.25	0.292(6)	0.038(6)	16	0.036
14	0.26	0.279(6)	—	8	0.027
20	0.27	0.266(6)	—	0	0.022
30	0.25	0.252(3)	—	0	0.014

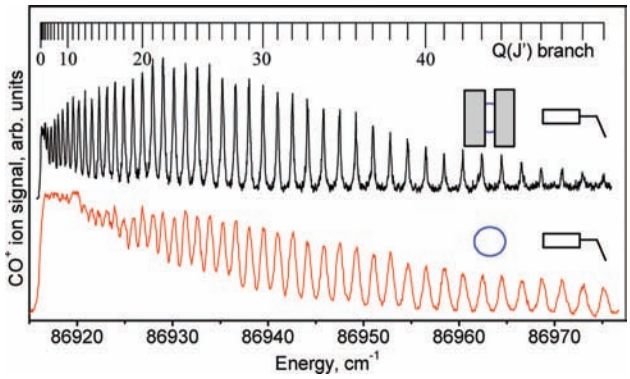

Figure 3. 2 + 1 REMPI spectra of the Q-branch of the B $^1\Sigma^+ \leftarrow$ X $^1\Sigma^+$ transition of CO from acetone dissociation at 230 nm. The Doppler-free spectrum shown in black was collected under the masked velocity mapping conditions. The Doppler-broadened spectrum recorded with the unmasked detector is shown in red.

not rely on the Doppler effect cancelation.[44–46] Our approach achieves laser line width limited resolution in detection simply by externally masking the phosphor screen under velocity map conditions in such a way that the products with no velocity component along the laser propagation direction are detected. For the population analysis, a simple mathematical procedure was then performed to transform the line intensities under masked detector conditions to the unmasked full ion cloud signal. A more detailed description of this method will be published elsewhere.[47] Figure 3 demonstrates a comparison between a Doppler-broadened REMPI B←X spectrum of CO acquired with the unmasked detector (red trace) and a Doppler-free spectrum recorded with the masked detector (black trace). The substantially improved resolution permitted us to observe that the spectrum peaks around $J'' = 22$ and allowed us to estimate that about 15% ± 5% of the total CO fragments are produced with the sharp $P(E_T)$ distribution. Here, the uncertainty is estimated based on reproducibility in our fitting procedure and the fact that we have only obtained images on a subset of all the rotational levels.

IV. Discussion

The broad translational energy release observed together with a wide range of rotational excitation of CO following 230 nm acetone photolysis is dynamically identical to the characteristics of the stepwise dissociation mechanism of bond cleavage in acetone previously studied at 193 and 248 nm. Trentelman et al.[48] carried out a thorough investigation of the 193 nm dissociation of acetone using rotationally resolved VUV-LIF excitation spectroscopy to detect CO. They observed considerable rotational excitation peaking around $J'' = 22$ for $v'' = 0$ of CO, which is in precise agreement with our results at 230 nm. The average translational energy value was determined to be 0.37 ± 0.05 eV by analyzing the Doppler profiles of several rovibronic transitions. North et al.[20] also performed a detailed investigation of the 193 photolysis of acetone using photofragment translational spectroscopy with universal detection of photodissociation products. Their average translational energy release value of 0.21 ± 0.03 eV is considerably lower. It should be noted that based on the perceptible deviation in rotational populations of the effusive and supersonic beam results for the $J''(CO) < 15$ data, Trentelman and co-workers[48] concluded that the excess population in low rotational states may originate from acetone clusters. Hence, it is possible that their translational energy measurements were performed for the $J'' > 15$ of CO,

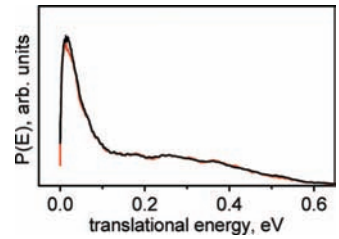

Figure 4. Nozzle temperature dependence of the $P(E)$ distributions for CO ($J'' = 5$). Experiments in which the temperature of the inlet tubing and nozzle were kept at 373 and 323 K are plotted correspondingly as black and red lines.

although not all of the rotational levels used for the analysis were specified. In any case, their result was a simple fit to Doppler-broadened lineshapes, and the laser line width contribution was significant in that case. Analysis of our bimodal distribution gives an average $\langle E_T \rangle$ around 0.24 eV, which is in good accord with measurements by North and co-workers. It should be noted that in this case comparing the average translational energies at the 193 and 230 nm photolysis is reasonable, as the translational energy release is likely dictated by the exit barrier heights in the primary and secondary dissociation steps, and insensitive to modest changes in available energy.

A question that immediately arises is why this slow component was not seen in the experiments of North et al. One obvious answer is that our result is at 230 nm, while the North result is at 193 nm. However, we believe the dynamics are similar at these wavelengths, so we are not satisfied with this explanation. In fact, the broad component in our distribution is in very good agreement with the 193 nm translational energy distribution North derived for CO, but overall there is strong deviation at the lowest energies, below 0.1 eV where the sharp peak begins to contribute. However, the photofragment translational spectroscopy (PTS) experiments are not sensitive to the slowest products, as they do not scatter far from the beam. The precise low energy limit will depend on the molecular beam velocity and the angles used in the analysis, and this is not entirely clear from the paper. It is thus possible that this slow component was present in the PTS experiments but that data sufficiently close to the beam was not recorded and fitted to reveal this contribution to the translational energy distribution. We should note that detection of $m/z = 28$ in the PTS experiments is extremely challenging, and the signal-to-noise achieved in that work already quite remarkable. Finally, although our average translational energy release is close to that given by North, it is somewhat larger, while the slow contribution would be expected to make it smaller. However, our result is for CO ($v'' = 0$) only, while theirs includes small contributions from higher vibrational levels, likely lowering the overall average.

Even though the stepwise dissociation mechanism has been previously studied in great detail, the sharp $P(E_T)$ distribution detected for CO with low rotational excitation has not been reported. The remainder of this discussion will be focused on identifying dissociation pathways that can lead to the low-J CO product with low, sharply peaked translational energy release.

In order to address the possibility that the bimodal distribution of the CO products originates from the dissociation of acetone clusters, the dependence of the $P(E_T)$ curves on nozzle temperature was examined. Figure 4 shows translational energy release at $J''(CO) = 5$ for the two sets of experiments differing only in the temperature of the inlet tubing and nozzle. The two $P(E_T)$ distributions are almost identical, implying that the contribution from the clusters is negligible.

An alternative source of the slow CO might be either a synchronous dissociation or unusual dynamics in the stepwise dissociation. For the former, based on momentum conservation we can readily estimate the translational energy imparted to the two methyl radicals. If we assume they depart simultaneously at the equilibrium bond angle for acetone, we find a translational energy of 0.065 eV in each methyl, also implying a total internal excitation of 6.3 eV in the methyl fragments. Although kinematically feasible, of course, there is no obvious mechanism to give rise to the simultaneous dissociation to highly vibrationally excited methyl radicals. As an alternative liming case, we can consider dissociation to ground-state methyl radicals and estimate the bond angle necessary to momentum match to CO. We find an angle of 96.8°, again calling for implausible dynamics rather difficult to justify. Finally, we can imagine stepwise dissociation with peculiar dynamics in the secondary dissociation causing the CO to be scattered back to the acetone center of mass, and in low rotational levels. Although it is possible to imagine this happening in some instances, it is very difficult to conceive of a reason for a distinct population of these events to happen with high probability.

As briefly mentioned in the Introduction, Zewail and co-workers[29,37] have argued that for sufficiently short photolysis wavelength (193 nm), instead of primary dissociation taking place on the T_1 surface ("T_1 mechanism"), direct decomposition on S_1 ("S_1 mechanism") may occur via a transition state that leads to a linear acetyl radical in the *A* state. Is the bimodal distribution in CO fragments then a sign of these two possible dissociation mechanisms: S_1 and T_1? In short, the answer is no. Given that the linear acetyl radical in the first electronically excited-state quickly relaxes to its ground state, as argued by Zewail and co-workers, the secondary decomposition fragments do not preserve memory of their S_1 or T_1 parentage. Therefore, the CO fragments from both mechanisms will have very similar energy partitioning, and no bimodal distribution is anticipated.

Another possible explanation that may account for the sharp $P(E_T)$ involves dissociation on the ground-state surface. According to ab initio calculations by Liu et al.[32] there is an S_1/S_0 intersection located at around 5.6 eV, which is very near the 230 nm photolysis energy used in this study. Furthermore, the S_1 transition state energy and geometry reported by Liu et al. is quite similar to that of this S_1/S_0 CI, making it likely for some molecules accessing this region of the surface to branch to the ground-state via internal conversion here. The dissociation on the ground-state is quite distinctive in that it occurs without a barrier to give CH_3 + acetyl. This is a necessary precondition for "roaming" dynamics. Given the barrierless dissocation, it is quite common for the system to attain a condition where there is almost but not quite enough energy in the reaction coordinate for radical dissociation. The methyl radical can then explore a wide flat region of the potential energy surface. This "near-dissociation" behavior of CH_3 radical may then eventually result in the intramolecular abstraction of the methyl group from CH_3CO radical to give excited ethane with CO, i.e., the roaming mechanism. The resulting CO fragments convey these distinct signatures of roaming as seen in the formaldehyde and acetaldehyde systems: very little translational energy release, low rotational excitation and high internal excitation of cofragments, which can be inferred from the $P(E_T)$ distributions if they can be resolved. For such complex molecules as acetone, we clearly do not expect to resolve the internal state distribution in the ethane cofragment as we do for H_2 in the formaldehyde case. However, other characteristics of the CO energy partitioning in acetone dissociation are dynamically analogous to those observed in photolysis of formaldehyde and acetaldehyde via roaming,[1,2,7,14] making roaming of methyl radical to give highly excited ethane, we believe, the most plausible explanation for the observed bimodal distribution of CO in acetone dissociation at 230 nm. An alternative ground-state dissociation pathway would be molecular decomposition via a three-center transition state (TS). To our knowledge, no such TS has been identified theoretically, although it is reasonable to assume one exists. However, such a TS leading to closed shell ethane and CO products would very likely have a high barrier, so the CO product would be expected to show high translational energy and high rotational excitation, inconsistent with what we see here.

There is perhaps additional support for this picture in the cell experiments involving isotopic mixtures discussed in the Introduction.[36] Those experiments, showing quite clear evidence for intramolecular ethane production following acetone dissociation in the near-ultraviolet, raise a number of interesting questions. The studies were conducted at energies below the threshold for triplet dissociation. In this case, it is possible that dissociation occurs via less efficient coupling to the ground-state than via the CI discussed above, perhaps via the triplet. Production of methyl radicals can then lead to intermolecular ethane formation as assumed by Pilling and co-workers.[19] However, roughly one-fourth of the ethane produced in the Russian study was attributed to an intramolecular reaction. In this case, it could be either by dissociation via a three-center transition state as mentioned above, or by a roaming mechanism as we have suggested. Although a TS pathway is certainly plausible, we are inclined to favor a roaming explanation in this case as well. The energy dependence shown in the formaldehyde system,[3,4] and the dominance of roaming in acetaldehyde,[9] suggest that when it is possible, the larger A-factor for the associated radical channel serves to favor roaming over the dissociation via the tight molecular TS. However, at this point it is little more than speculation concerning the results in the near UV. At 230 nm, however, our results bear the clear sign of roaming in the CO quantum state-specific translational energy distributions.

The final question then is the fate of the ethane. We can readily estimate the internal energy in the ethane produced in a roaming event following 230 nm acetone dissociation to give low-*J* CO with 0.038 eV translational energy: it is over 5 eV. This is well above the dissociation energy of ethane back to $CH_3 + CH_3$, as well as to $C_2H_5 + H$ or $C_2H_4 + H_2$. We thus do not anticipate any bound ethane to result from this reaction under collisionless conditions. We should note that Pilling and co-workers saw no evidence that would contradict this roaming contribution to their observed ethane production at 193 nm,[19] as the ethane end-product, even from the roaming case, would arise ultimately via recombination of methyl radicals that could be quenched by a radical scavenger. Furthermore, they clearly saw a nonscavengeable ethylene product, although they did not give a compelling explanation for it. In any case, if roaming is indeed occurring in acetone photodissociation, we expect to see it in a reallocation of the product momenta and the opening of these otherwise surprising channels such as ethyl radical or ethylene production. Despite decades of study of acetone photochemistry, more theoretical and experimental work is clearly needed.

Acknowledgment. We are grateful to Prof. S. North for valuable discussions. This work was supported by the Director, Office of Science, Office of Basic Energy Science, Division of

Chemical Science, Geoscience and Bioscience, of the U.S. Department of Energy under Contract No. DE-FG02-04ER15593.

References and Notes

(1) Townsend, D.; Lahankar, S. A.; Lee, S. K.; Chambreau, S. D.; Suits, A. G.; Zhang, X.; Rheinecker, J.; Harding, L. B.; Bowman, J. M. Science 2004, *306*, 1158.

(2) Lahankar, S. A.; Chambreau, S. D.; Townsend, D.; Suits, F.; Farnum, J.; Zhang, X.; Bowman, J. M.; Suits, A. G. *J. Chem. Phys.* **2006**, *125*, 044303.

(3) Lahankar, S. A.; Chambreau, S. D.; Zhang, X.; Bowman, J. M.; Suits, A. G. *J. Chem. Phys.* **2007**, *126*, n/a.

(4) Lahankar, S. A.; Goncharov, V.; Suits, F.; Farnum, J. D.; Bowman, J. M.; Suits, A. G. *Chem. Phys.* 2007, doi: 10.1016/ j.chemphys.2007.11.007.

(5) Zhang, X.; Rheinecker, J. L.; Bowman, J. M. *J. Chem. Phys.* **2005**, *122*, 114313.

(6) Rheinecker, J. L.; Zhang, X.; Bowman, J. M. *Mol. Phys.* **2005**, *103*, 1067.

(7) Houston, P. L.; Kable, S. H. *Proc. Natl. Acad. Sci. U.S.A.* **2006**, *n/a*, n/a.

(8) Harding, L. B.; Klippenstein, S. J.; Jasper, A. W. *Phys. Chem. Chem. Phys.* **2007**, *31*, 4055.

(9) Shepler, B. C.; Braams, B. J.; Bowman, J. M. *J. Phys. Chem. A* **2007**, *111*, 8282.

(10) Hase, W. L.; Hu, X. *Chem. Phys. Lett.* **1989**, *156*, 115.

(11) Lopez, J. G.; Vayner, G.; Lourderaj, U.; Addepalli, S. V.; Kato, S.; Dejong, W. A.; Windus, T. L.; Hase, W. L. *J. Am. Chem. Soc.* **2007**, *129*, 9976.

(12) Mann, D. J.; Hase, W. L. *J. Am. Chem. Soc.* **2002**, *124*, 3208.

(13) Pomerantz, A. E.; Camden, J. P.; Chiou, A. S.; Ausfelder, F.; Chawla, N.; Hase, W. L.; Zare, R. N. *J. Am. Chem. Soc.* **2005**, *127*, 16368.

(14) Rubio-Lago, L.; Amaral, G. A.; Arregui, A.; Izquierdo, J. G.; Wang, F.; Zaouris, D.; Kitsopoulos, T. N.; Banares, L. *Phys. Chem. Chem. Phys.* **2007**, *9*, 6123.

(15) Badr, Y.; El-Wanees, S. A.; Mahmoud, M. A. *J. Photochem. Photobiol. A−Chem.* **2004**, *167*, 159.

(16) Berrie, C. L.; Longfellow, C. A.; Suits, A. G.; Lee, Y. T. *J. Phys. Chem. A* **2001**, *105*, 2557.

(17) Donaldson, D. J.; Leone, S. R. *J. Chem. Phys.* **1986**, *85*, 817.

(18) Hall, G. E.; Metzler, H. W.; Muckerman, J. T.; Preses, J. M.; Weston, R. E. *J. Chem. Phys.* **1995**, *102*, 6660.

(19) Lightfoot, P. D.; Kirwan, S. P.; Pilling, M. J. *J. Phys. Chem.* **1988**, *92*, 4938.

(20) North, S. W.; Blank, D. A.; Gezelter, J. D.; Longfellow, C. A.; Lee, Y. T. *J. Chem. Phys.* **1995**, *102*, 4447.

(21) Takahashi, K.; Nakayama, T.; Matsumi, Y.; Osamura, Y. *J. Phys. Chem. A* **2004**, *108*, 8002.

(22) Kim, S. K.; Pedersen, S.; Zewail, A. H. *J. Chem. Phys.* **1995**, *103*, 477.

(23) Buzza, S. A.; Snyder, E. M.; Card, D. A.; Folmer, D. E.; Castleman, A. W. *J. Chem. Phys.* **1996**, *105*, 7425.

(24) Buzza, S. A.; Snyder, E. M.; Castleman, A. W. *J. Chem. Phys.* **1996**, *104*, 5040.

(25) Owrutsky, J. C.; Baronavski, A. P. *J. Chem. Phys.* **1998**, *108*, 6652.

(26) Owrutsky, J. C.; Baronavski, A. P. *J. Chem. Phys.* **1999**, *110*, 11206.

(27) Zhong, Q.; Poth, L.; Castleman, A. W. *J. Chem. Phys.* **1999**, *110*, 192.

(28) Diau, E. W. G.; Kotting, C.; Zewail, A. H. *Chemphyschem* **2001**, *2*, 273.

(29) Chen, W. K.; Ho, J. W.; Cheng, P. Y. *Chem. Phys. Lett.* **2003**, *380*, 411.

(30) Chen, W. K.; Cheng, P. Y. *J. Phys. Chem. A* **2005**, *109*, 6818.

(31) Chen, W. K.; Ho, J. W.; Cheng, P. Y. *J. Phys. Chem. A* **2005**, *109*, 6805.

(32) Liu, D.; Fang, W. H.; Fu, X. Y. *Chem. Phys. Lett.* **2000**, *325*, 86.

(33) Martinez-Nunez, E.; Fernandez-Ramos, A.; Cordeiro, M.; Vazquez, S. A.; Aoiz, F. J.; Banares, L. *J. Chem. Phys.* **2003**, *119*, 10618.

(34) Diau, E. W. G.; Kotting, C.; Solling, T. I.; Zewail, A. H. *Chemphyschem* **2002**, *3*, 57.

(35) North, S.; Blank, D. A.; Lee, Y. T. *Chem. Phys. Lett.* **1994**, *224*, 38.

(36) Skorobogatov, G. A.; Meilakhs, A. G.; Pogosyan, Y. U.; Khripun, V. K. *Russ. J. Gen. Chem.* **2002**, *72*, 1271.

(37) Solling, T. I.; Diau, E. W. G.; Kotting, C.; De Feyter, S.; Zewail, A. H. *Chemphyschem* **2002**, *3*, 79.

(38) Townsend, D.; Minitti, M. P.; Suits, A. G. *Rev. Sci. Instrum.* **2003**, *74*, 2530.

(39) Huang, C.; Li, W.; Kim, M. H.; Suits, A. G. *J. Chem. Phys.* **2006**, *125*, 121101/1.

(40) Cunshun, H.; Armando, D. E.; Arthur, G. S. *J. Chem. Phys.* **2008**, *128*, 134301.

(41) Li, W.; Chambreau, S. D.; Lahankar, S. A.; Suits, A. G. *Rev. Sci. Instrum.* **2005**, *76*, 063106/1.

(42) Muckerman, J. T. *J. Phys. Chem.* **1989**, *93*, 179.

(43) Goncharov, V.; Vasyutinskii, O. V.; Herath, N.; Suits, A. G. In preparation.

(44) Vasilenko, L. S.; Chebotaev, V. P.; Shishaev, A. V. *ZhETP Pis. Red.* **1970**, *12*, 161.

(45) Levenson, M. D.; Bloembergen, N. *Phys. Rev. Lett.* **1974**, *32*, 645.

(46) Biraben, F.; Cagnac, B.; Grynberg, G. *Phys. Rev. Lett.* **1974**, *32*, 643.

(47) Goncharov, V.; Herath, N.; Suits, A. G. Manuscript in progress.

(48) Trentelman, K. A.; Kable, S. H.; Moss, D. B.; Houston, P. L. *J. Chem. Phys.* **1989**, *91*, 7498.

JP802534R